ATOMS, SPECTRA, RADIATION

Zeeman Laser Cooling of 85Rb Atoms in Transverse Magnetic Field

P. N. Melentiev, P. A. Borisov, and V. I. Balykin

Institute of Spectroscopy, Russian Academy of Sciences, Troitsk, Moscow oblast, 142190 Russia
e-mail: melentiev@isan.troitsk.ru
Received August 7, 2003

Abstract—The process of Zeeman laser cooling of 85Rb atoms in a new scheme employing a transverse magnetic field has been experimentally studied. Upon cooling, the average velocity of atoms was 12 m/s at a beam intensity of 7.2×10^{12} s^{-1} and an atomic density of 4.7×10^{10} cm^{-3}. © *2004 MAIK "Nauka/Interperiodica".*

1. INTRODUCTION

Cold atomic beams characterized by a small average velocity of atoms at a high intensity and high phase space density are widely used in various experiments in atomic beam optics, interferometry, and lithography [1, 2]. Low-energy atomic beams can be obtained by method of laser cooling, which is known in several variants employing the Zeeman effect [3, 4], frequency-chirped laser radiation [5], isotropic light [6], and wideband laser radiation [7]. Unfortunately, the process of cooling by all these techniques is accompanied by unavoidable increase in the transverse temperature of atoms and, hence, by a decrease in the beam brightness and phase space density.

An effective means of solving this problem is offered by schemes employing a two-dimensional magneto-optical trap (2D-MOT) ensuring both transverse compression of the atomic beam and a decrease in the transverse velocity of atoms [8–10]. The degree of compression and cooling in 2D-MOT is usually limited by a finite time of flight of atoms through the apparatus. Effective use of 2D-MOTs requires that atoms in a beam would possess a sufficiently low longitudinal velocity.

An alternative method for obtaining atomic beams of high brightness and high phase space density is based on the extraction of atoms from a three-dimensional MOT (3D-MOT) [11], an advantage of this device being a relatively high phase space density of atoms. However, the use of this technique for obtaining continuous atomic beams of high intensity is limited by the large time required for the accumulation of atoms.

We have developed a new method for obtaining cold atomic beams of high intensity (7.2×10^{12} s^{-1}) and a small average velocity of atoms (12 m/s) and have studied this method in application to a beam of 85Rb atoms. The proposed technique employs the Zeeman laser cooling of thermal 85Rb atoms in *transverse* magnetic

field [12]. Application of the *transverse* magnetic field allowed us to obtain the optimum distribution of magnetic field along the beam axis, which is necessary for effective cooling. Using the scheme with transverse magnetic field, we succeeded in creating a compact and effective Zeeman slower ensuring the formation of intense beams of atoms with an average velocity as low as 10 m/s.

2. ZEEMAN LASER COOLING

2.1. Zeeman Slowing in Longitudinal Magnetic Field

According to the method of laser cooling, an atomic beam interacts with the counterpropagating beam of laser radiation with a frequency tuned in resonance with that of a given atomic transition. In the course of deceleration, the absorption frequency exhibits a Doppler shift relative to the laser radiation frequency and, hence, the efficiency of the process tends to decrease. The Doppler shift can be compensated using the linear Zeeman effect. The scheme of atomic beam cooling by laser radiation in a magnetic field, called Zeeman slowing, is now most widely used for obtaining slow atomic beams.

An experimental setup for Zeeman slowing comprises a source of neutral atoms and a Zeeman slower creating the required magnetic field distribution in the zone of interaction between atoms and laser radiation. The cooling laser radiation tuned in resonance with a given atomic transition propagates in the direction opposite to that of the atomic beam. In most Zeeman slower schemes, atoms are decelerated only inside the apparatus and do not interact with the laser radiation outside. The required magnetic field configuration in the Zeeman slower is created using a magnetic solenoid with the distance between turns varied so as to provide
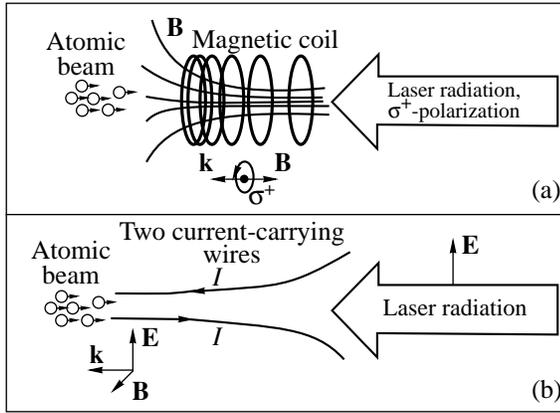
Fig. 1. Schematic diagrams illustrating Zeeman laser cooling of an atomic beam in (a) longitudinal and (b) transverse magnetic fields.

for the optimum distribution of the magnetic field in the axial direction. The solenoid axis coincides with the axes of atomic and laser beams (Fig. 1a). It is possible to use ring permanent magnets instead of the magnetic coil. In both cases, the magnetic field vector in the Zeeman slower is collinear with the wavevector of laser radiation. The laser radiation possesses a σ^+ polarization and excites transitions between the Zeeman sublevels corresponding to a change in the magnetic quantum number $\Delta m = +1$.

The Zeeman shift of the atomic transition frequency is proportional to the magnetic field strength (magnetic induction) B: $\Delta\omega_{\text{Zeeman}} = \alpha B$, where α is a constant determined by the Zeeman effect. The resonance interaction between atoms and laser radiation in the Zeeman slower is determined by the condition

$$\Delta + kV - \alpha B = 0, \tag{1}$$

where $\Delta = \omega_{\text{laser}} - \omega_0$ is the detuning of the laser radiation frequency ω_{laser} from the atomic transition frequency ω_0 in a zero magnetic field, V is the atomic velocity, and $k = 2\pi/\lambda$ is the wavevector. If the magnetic field B varies in space so that condition (1) is valid at all points of the atomic trajectory in the course of deceleration, then atoms occur in resonance with the laser radiation.

The required magnetic field distribution in the Zeeman slower can be readily determined as follows. When condition (1) is fulfilled at all points of the atomic trajectory, the force of light pressure imparts a constant acceleration a to an atom so that its velocity decreases according to the law

$$V(z) = \sqrt{V_0^2 - 2az}.$$

The acceleration is determined by the expression

$$a = \frac{\hbar k \Gamma}{2M} \frac{G}{1 + G + (\Delta + kV - \alpha B)^2/\gamma^2}, \tag{2}$$

where 2γ is the natural width of the given atomic transition, M is the atomic mass, $G = I/I_{\text{sat}}$ is the parameter of saturation of the atomic transition, I is the laser radiation intensity, and I_{sat} is the laser saturation intensity. The latter quantity is given by the formula

$$I_{\text{sat}} = \frac{\hbar \omega_0}{2\tau\sigma}, \tag{3}$$

where $\tau = 1/2\gamma$ is the time of spontaneous decay and ω_0 is the atomic transition frequency, and σ is the absorption cross section.

Let the laser frequency be tuned precisely in resonance to that of the given atomic transition. Using condition (1), we obtain an expression for the required field profile:

$$B(z) = B_0 \sqrt{1 - \frac{2az}{V_0^2}}.$$

The existence of a maximum possible acceleration for a given atom in a magnetic field, $a_{\text{max}} = 2\hbar k\Gamma/M$ (for $I \gg I_{\text{sat}}$) poses a limitation on the maximum magnetic field gradient [3],

$$\left(\frac{dB}{dz}\right)_{\text{max}} \le \left(\frac{dB}{d\omega}\right)\frac{a_{\text{max}}}{\lambda V}, \tag{4}$$

where $dB/d\omega = \alpha^{-1}$. When the magnetic field gradient is below maximum, the laser radiation intensity is limited by the condition

$$G \ge \frac{1}{1 + \dfrac{a_{\text{max}}}{V\lambda}\dfrac{dB}{d\omega}\dfrac{dz}{dB}}. \tag{5}$$

The minimum temperature T_{D} of atoms that can be achieved by means of Zeeman slowing, called the Doppler cooling limit, is determined by the formula [13]

$$T_{\text{D}} = \frac{\hbar\gamma}{2k_B}. \tag{6}$$

For ^{85}Rb atoms, $T_{\text{D}} = 141$ μK and the corresponding minimum atomic velocity is $V_{\text{D}} = 0.12$ m/s. However, there are several other limiting factors that hinder obtaining such a low velocity by Zeeman slowing. The main difficulty is encountered in extracting low-energy

atoms from the Zeeman slower [4]: at a low atomic velocity (~10 m/s), the length of interaction between an atom and the laser field on which the velocity is reversed is as small as a fraction of a millimeter. For this reason, intense atomic beams with particle velocities below 50 m/s could not be obtained by means of Zeeman slowing.

2.2. Zeeman Slowing
in a Transverse Magnetic Field

The principal difference between the Zeeman slowing in a *transverse* magnetic field and the scheme considered above is that the magnetic field vector is perpendicular to the wavevector of the cooling laser radiation (in the conventional scheme, these vectors are collinear). This mutual orientation of the magnetic field **B** and the wavevector **k** determines, in turn, the required polarization of the laser radiation, and the electric field vector is perpendicular to the magnetic field vector **B** (Fig. 1b). In this configuration, the laser radiation can induce atomic transitions with a change in the magnetic quantum number $\Delta m = +1$ or $\Delta m = -1$.

The method of Zeeman slowing in the transverse magnetic field offers two important advantages over the conventional scheme: (i) simpler realization of the required magnetic field distribution in the Zeeman slower and (ii) higher accuracy of controlling the length of interaction between atoms and laser radiation, facilitating the extraction of low-energy atoms from the Zeeman slower. Let us consider application of the new scheme to cooling ^{85}Rb atoms.

The existence of hyperfine splitting of the ground and excited states in alkali metal atoms leads to transitions between various sublevels of the hyperfine structure. Excitation with single-mode laser radiation leads to optical pumping of atoms to one sublevel of the hyperfine structure of the ground state and drives these atoms out of resonance with the laser radiation. For ^{85}Rb atom (Fig. 2), a transition from the ground state with $F = 3$ to an excited state with $F' = 4$ is a cyclic transition and the $F' = 4 \longrightarrow F = 2$ transition is forbidden in the dipole approximation. Therefore, the former transition can be used for Zeeman slowing of ^{85}Rb atoms.

However, there is a small probability (6×10^{-4} for a laser intensity on a saturation level) of a transition to the sublevel with $F' = 3$ of the excited state. From this state, the atom can equiprobably pass either to the ground state sublevel with $F = 3$ or to an excited sublevel with $F = 2$ spaced at 3 GHz from the sublevel with $F = 3$, which will break cyclic interaction with the laser radiation. A commonly accepted straightforward solution of this problem consists in using two-frequency laser radiation. The dominant (cooling) laser mode (decelerating
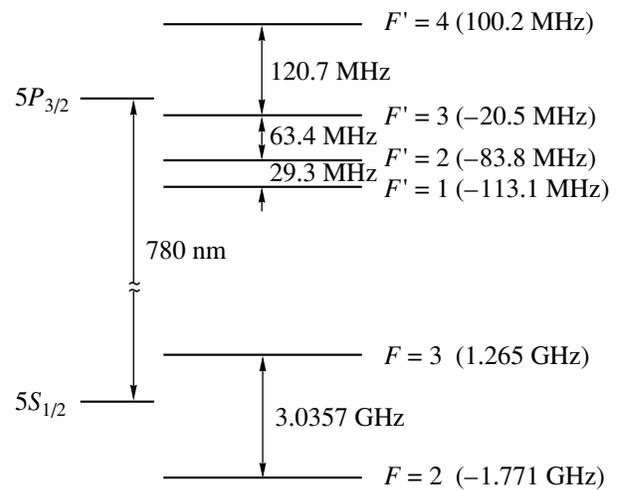

Fig. 2. Schematic diagram of energy levels of the D_2 line of ^{85}Rb atom.

field) is tuned in resonance to the $F = 3 \longrightarrow F' = 4$ transition. The second (auxiliary) mode is tuned in resonance to the $F = 2 \longrightarrow F' = 3$ transition so as to provide for the optical pumping of the ground state sublevel with $F = 3$.

For ^{85}Rb atoms possessing thermal velocities, a Doppler frequency shift is greater than the distance between sublevels of the hyperfine structure of an excited state. For this reason, the positions of energy levels in a magnetic field should be calculated for the cases of weak and strong magnetic fields. In a weak magnetic field, each component of the hyperfine structure of the ground and excited states of ^{85}Rb atom splits into $2F + 1$ Zeeman sublevels characterized by the magnetic quantum number m_F,

$$U_{m_F} = \mu_B g_F m_F B, \tag{7}$$

where $\mu_B = 9.27 \times 10^{-24}$ J/T is the Bohr magneton and g_F is the Lande factor.

In strong magnetic fields such that the energy of an atom in the magnetic field is greater than the energy of electron interaction with the nucleus, the character of splitting changes significantly. A level characterized by the magnetic quantum number J splits into $(2J + 1)(2I + 1)$ sublevels, determined by the quantum numbers m_I and m_J, with the energies

$$U_{m_J m_I} = \mu_B g_J m_J B + A m_I m_J, \tag{8}$$

where A is the hyperfine splitting constant. For the $5P_{3/2}$ level of ^{85}Rb atom, $A = 25$ MHz.

Figure 3 shows the pattern of splitting of the magnetic sublevels of the ground ($5S_{1/2}$) and excited ($5P_{3/2}$) states of ^{85}Rb atom in a magnetic field B. As can be
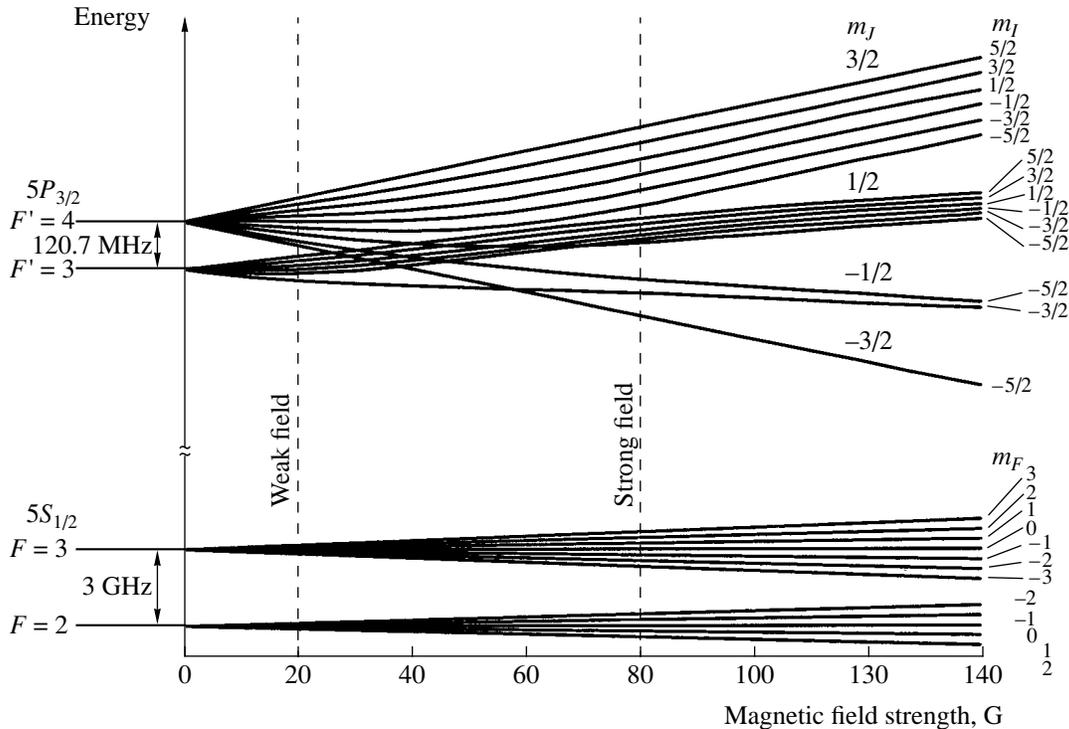
Fig. 3. The hyperfine structure of energy levels of the ground ($5S_{1/2}$) and excited ($5P_{3/2}$) states (the levels with $F' = 3, 4$) of ^{85}Rb atom in a magnetic field.

seen, the weak magnetic field approximation is valid for most of the sublevels under consideration in a field with $B < 20$ G, while the strong magnetic field approximation is applicable when $B > 80$ G.

For the ground state level with $F = 2$, the Lande factor is negative, while for the level with $F = 3$ this factor is positive. As a result, the Zeeman sublevels of the ground state levels with the same magnetic moment projection m_F behave differently in response to increasing magnetic field strength. As can be seen from Fig. 3, the field dependences of the frequencies of transitions between magnetic sublevels with $F = 3$ and $F' = 4$ significantly differ from the analogous dependences for the states with $F = 2$ and $F' = 3$. Since the Doppler shift for these levels is the same, the complicated behavior of magnetic sublevels in the applied magnetic field will lead to a loss in efficiency of excitation for the second mode of the two frequency laser radiation in the course of Zeeman slowing. The efficiency in interaction between atoms and laser radiation can be increased at the expense of the field-induced broadening. According to our calculations, the parameters G_1 and G_2 of the atomic transition saturation for the dominant (cooling) laser mode and the second (auxiliary) mode, respectively, must obey the condition $G_2 \geqslant 0.1G_1$.

When ^{85}Rb atoms interact with a two frequency laser radiation in the presence of a magnetic field, several photon absorption–reemission cycles are sufficient for the optical pumping of the atom to the sublevels with $F = 3, m_F = 3$ and $F = 2, m_F = 2$. Therefore, an analysis of the Zeeman slowing can be restricted to the $F = 3, m_F = 3 \longrightarrow F' = 4, m_F = 4$ and $F = 2, m_F = 2 \longrightarrow F' = 3, m_F = 3$ transitions.

The number of cooled atoms at the output of the Zeeman slower is, together with the average velocity of atoms, among the most important parameters characterizing the cooling efficiency. This number is determined primarily by two factors: (i) the fraction of the initial velocity distribution of atoms cooled by laser radiation in the Zeeman slower and (ii) the fraction of the primary atomic flux injected into the Zeeman slower. The former circumstance dictates the need for increasing the velocity interval of atoms subjected to cooling. However, this usually leads to a considerable increase in the length of the Zeeman slower and, accordingly, to a decrease in the flux of thermal atoms injected into the system. An analysis shows that the shorter the Zeeman slower, the greater the output flux of cold atoms. In selecting the optimum Zeeman slower length, it is also necessary to take into account the fact that the real atomic velocity distribution in a beam is depleted of the low-velocity fraction because of atomic collisions in the beam [14]. With allowance for this fact, we selected a magnetic field configuration in the Zeeman slower such that atoms are decelerated beginning
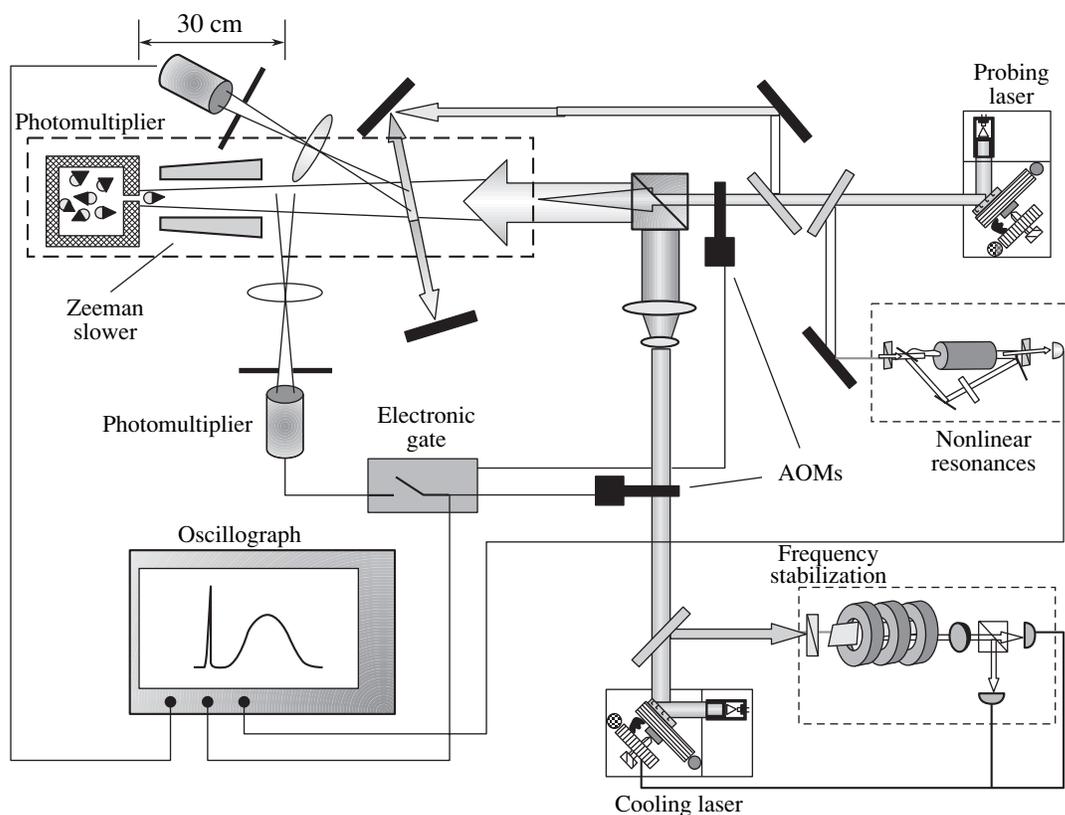
Fig. 4. Schematic diagram of the experimental setup.

3. EXPERIMENTAL SETUP

The experimental setup for studying the Zeeman slowing of atoms is schematically depicted in Fig. 4. The radiation sources were semiconductor lasers employing the Littrov scheme. Both lasers operated in a two frequency lasing regime ensured by resonance excitation of the relaxation oscillations due to microwave modulation of the injection current [15]. The microwave modulation frequency was equal to the difference in the frequencies of $F = 3 \longrightarrow F' = 4$ and $F = 2 \longrightarrow F' = 3$ transitions (2916 MHz). The microwave generator power was selected such that the intensity at the fundamental frequency would be four times that of the first side band. The dominant laser mode was used to excite the $F = 3 \longrightarrow F' = 4$ transition in ^{85}Rb atoms, while the one at the side band frequency excited the $F = 2 \longrightarrow F' = 3$ transition. The maximum laser output power was 15 mW. The laser beam diameter at the Zeeman slower entrance and exit was 3.5 and 5 mm, respectively. The cooling lasers were operating in the regime of active frequency stabilization with respect to the absorption signal in a cell placed in the magnetic field [16]. The short-term laser frequency stability was 3 MHz, while the long-term frequency drift was within

9 MHz/h. The probing laser frequency was chirped in the vicinity of the frequency of the $F = 3 \longrightarrow F' = 4$ transition in ^{85}Rb. The atomic velocity distribution was determined using the signal of fluorescence detected by a photomultiplier.

In order to eliminate the influence of the cooling laser radiation during the atomic velocity measurements, the cooling laser was switched off by means of an acoustooptical modulator (AOM). The fluorescence signal was measured using a BoxCar electronic gate (Fig. 5). In order to determine a stationary distribution of the atomic velocities, the time for which the cooling laser was switched on was selected sufficiently large, so that slow atoms leaving the slower could reach the detector before the laser was switched off. In our experimental configuration, this time was 6 ms. With this time delay, we measured the stationary distribution of atomic velocities—the same as that established for the constant laser irradiation of the atomic beam. In order to reduce the mechanical action upon atoms from the side probe laser, the probing laser radiation was switched on by an AOM only during the fluorescence measurements.

Since we employed the low-velocity part of the initial atomic velocity distribution for laser cooling, special measures were taken to obtain a beam of thermal atoms with undepleted low-energy fraction of the total
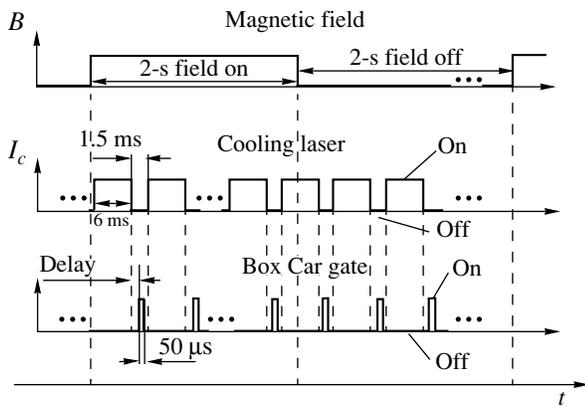
Fig. 5. Time series of the switching of magnetic field $B(t)$, cooling laser field $I_c(t)$, and BoxCar gate for monitoring the atomic velocity distribution during Zeeman slowing.

velocity distribution. This was achieved by using a source of ^{85}Rb atoms analogous to that described in [17]. The atomic source temperature could be varied from 20 to 500°C. The intensity of the atomic beam formed with a 4-mm aperture at a source temperature of $T = 250$°C was 4.5×10^{13} s^{-1} (approximately half of the

calculated value). Investigation of the primary atomic beam characteristics showed that this source exhibited no depletion of the low-energy part of the velocity distribution as a result of the beam scattering from vapor in the vicinity of the exit diaphragm of the atomic oven.

The magnetic field profile along the Zeeman slower axis was calculated using the formula

$$B(z) = B_0 \sqrt{1 - \frac{a_{max} z}{V_0^2}},$$

where $a_{max} = 1.07 \times 10^5$ m/s^2 and the initial velocity is $V_0 = 150$ m/s. The Zeeman slower comprised two 22-cm-long aluminum stripe combs cut to various depths (Fig. 6). The variable cut depth allowed the required field profile along the axis to be obtained because the current passed only via a continuous part of the metal stripe. The comb configuration provided for an increase in the effective mass and the surface area, thus increasing the heat exchange rate under ultrahigh vacuum conditions.

Figure 7 compares the calculated and experimentally measured field profiles along the Zeeman slower axis for a current of $I = 170$ A. As can be seen, the max-
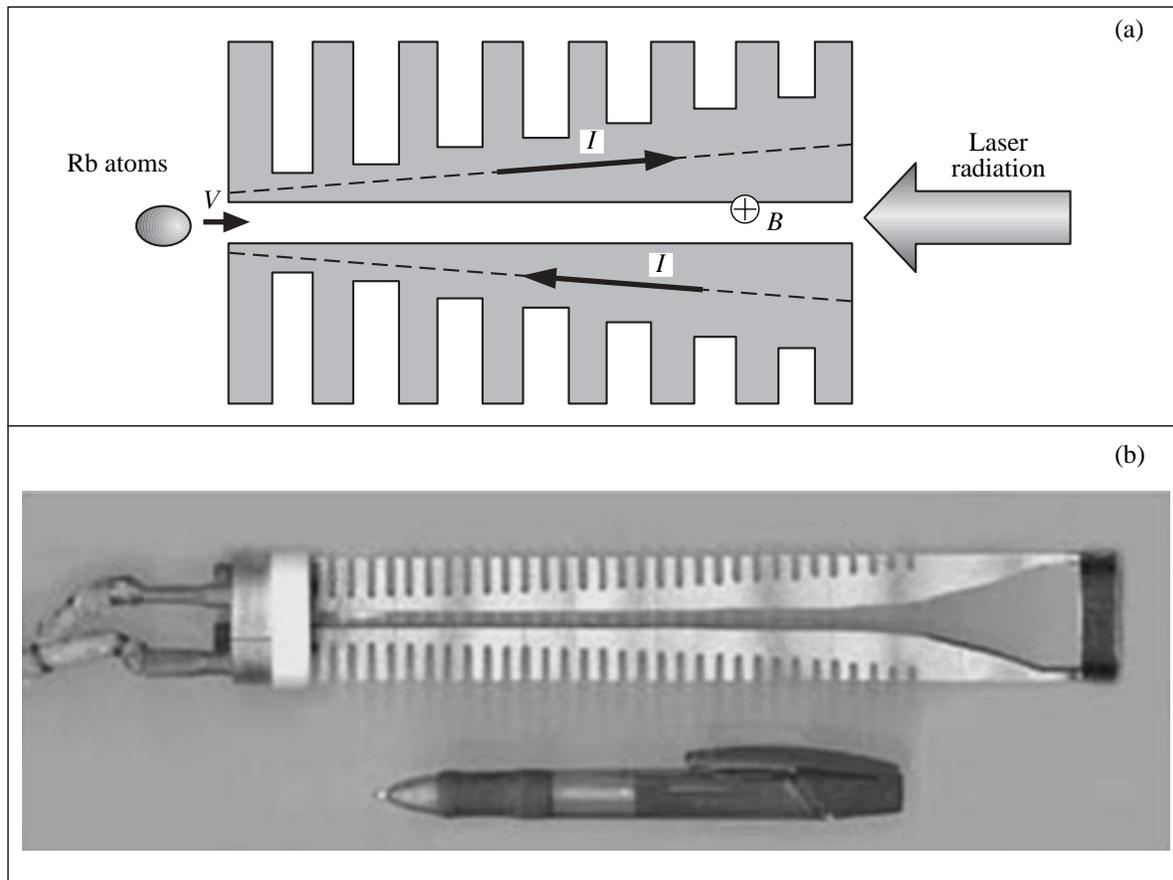

Fig. 6. The Zeeman slower: (a) schematic diagram; (b) general view.

imum deviation of the measured magnetic field strength from the calculated profile amounts to $\Delta B = 15$ G. This deviation may lead to a decrease in the Zeeman slowing efficiency as a result of the laser radiation being out of resonance with the atomic transition frequency. The compensation of the deviation of the magnetic field strength from that required for the effective cooling was achieved by increasing the laser radiation intensity. To this end, the parameter of the atomic transition saturation must be not less than

$$G \approx 14.$$

The electric resistance of the Zeeman slower (together with connecting leads in the vacuum chamber) was $R = 3 \times 10^{-3}$ Ω. For a current of 170 A passing through the device, the electric power converted into heat amounted to 90 W. In order to reduce the influence of Joule heating of the Zeeman slower on the residual gas pressure in the vacuum chamber, the current was supplied in a quasiperiodic regime, with the current switched on for 2 s and off for 8 s. The residual gas pressure in the vacuum chamber was 3×10^{-7} Torr.

For a correct analysis of the measured atomic velocity distributions, it is very important to know the position of zero velocity. For this purpose, a part of the probing laser radiation was introduced perpendicularly to the atomic beam and the corresponding fluorescence component was measured by a separate photomultiplier. Since this scheme eliminates the Doppler broadening, the resonance between the atomic fluorescence signal and the probing radiation indicated the position of the exact resonance corresponding to the $F = 3 \longrightarrow F' = 4$ transition, thus determining the atoms with a zero velocity. It should be noted that deviation of the angle between the probing laser radiation and the atomic beam from $90°$ leads to an error in the zero velocity determination. In order to minimize this error, the probing laser radiation was adjusted to cross the atomic beam at an angle of about $89°$ and reflected back by a mirror. This resulted in the appearance of two peaks equally shifted from the zero velocity position. The accuracy of zero velocity calibration in this scheme is determined by the uncertainty of matching of the forward and reflected laser beams. In our experiments, this uncertainty led to an error below 2 m/s in the velocity determination. We have also used an alternative technique for the zero velocity calibration based on the monitoring of nonlinear absorption resonances in a cell with Rb vapor.

4. EXPERIMENTAL RESULTS

Figure 8 shows the atomic velocity distributions of a beam of ^{85}Rb atoms upon Zeeman slowing at various detunings Δ of the laser radiation frequency. The atomic source temperature was $T = 250°$C. A peak in the low-velocity part of the distribution corresponds to
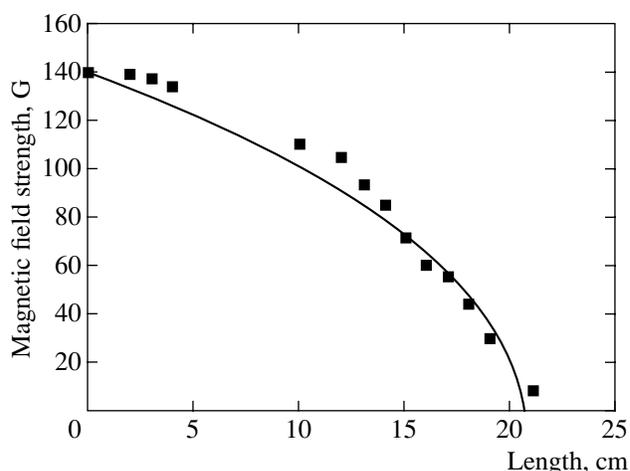
Fig. 7. Magnetic field distribution along the Zeeman slower axis. Solid curve shows the ideal calculated profile; squares show the experimental data.
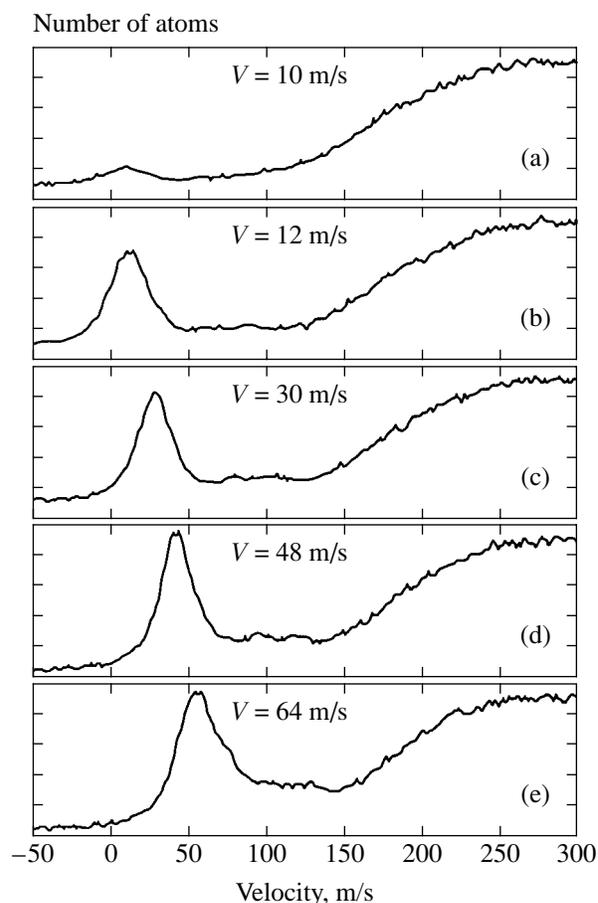
Fig. 8. The velocity distribution of ^{85}Rb atoms in a beam upon Zeeman slowing for various detunings of the cooling laser frequency Δ (MHz): (a) –39, (b) –46, (c) –54, (d) –66, (e) –77.

atoms decelerated as a result of the Zeeman slowing. As can be seen from these data, the average velocity of atoms in this peak, as well as the peak amplitude, depend on the laser frequency detuning. The closer the
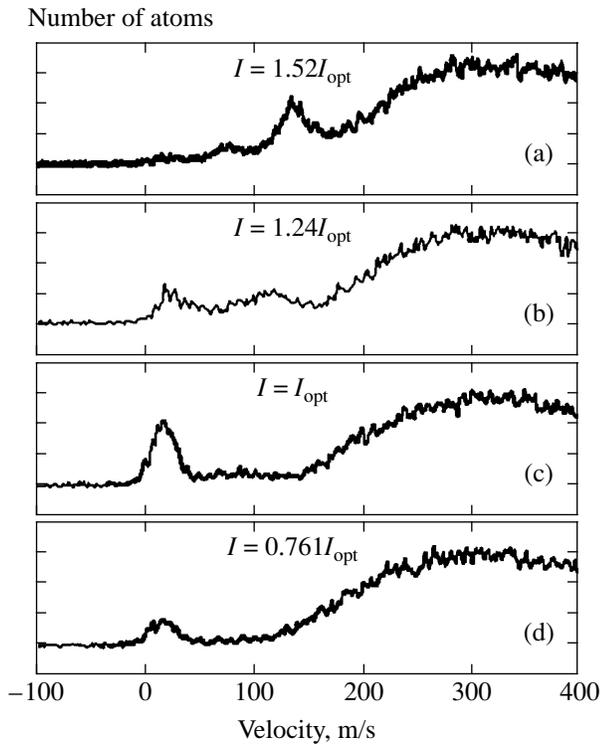
Number of atoms

Fig. 9. The effect of magnetic field strength in the Zeeman slower on the atomic velocity distribution. The maximum cooling efficiency is observed for the magnetic field induced by the current $I = I_{opt} = 170$ A.

cooling laser frequency to that of the atomic transition, the lower the average velocity of cooled atoms.

The data in Fig. 8 show that the amplitude of the peak of cold atoms remains virtually unchanged for the laser frequency detunings corresponding to the average velocities of cooled atoms above $V = 12$ m/s. The peak of cold atoms accounts for about 7% of the total number of atoms in the initial velocity distribution, which agrees with theoretical estimates. For the average velocity below 12 m/s, the peak amplitude drops with decreasing detuning Δ. A minimum average velocity for which the peak contains a significant fraction of atoms from the initial distribution is 10 m/s ($\Delta = -39$ MHz). This decrease in the low-velocity peak amplitude is explained by a decrease in the efficiency of detection of low-energy atoms, which is caused by a large divergence of the beam of atoms with longitudinal velocities below 15 m/s. Good agreement of the experimentally observed numbers of cooled atoms with the results of calculations showed that the proposed scheme provides for the effective extraction of cold atoms from the Zeeman slower.

In the spectra of Fig. 8, a full width at half maximum (FWHM) of the peak of cold atoms amounts to $\Delta V = 28 \pm 2$ m/s. This value is significantly greater than the minimum width determined by the Doppler cooling limit. There are several factors responsible for the final

(and higher than the Doppler limit) temperature of the atomic beam. According to the results of our calculations, spatial inhomogeneity of the laser radiation intensity leads to a finite width of the atomic velocity distribution on a level of 6 m/s, spatial inhomogeneity of the magnetic field leads to additional broadening of about 3 m/s, and a contribution due to the impulse diffusion amounts to 0.5 m/s. The total calculated width of the low-velocity peak is $\Delta V \approx 10$ m/s, which corresponds to a temperature of $\Delta T \approx 1$ K. This estimate is lower than the value observed in experiment. The discrepancy is related to a finite length of the detection zone, in which atoms continue to interact with the cooling laser radiation. As a result, the average velocity of atoms at various points of the detection zone exhibits various values.

In order to study the dependence of the slowing efficiency on the magnetic field strength in the Zeeman slower, we varied the current passing through the system, all other parameters being fixed. The corresponding velocity spectra are presented in Fig. 9. As can be seen, the curves measured for the current exceeding $I_{opt} = 170$ A exhibit two peaks. This is related to the fact that the process at high currents does not obey the condition (4) for the maximum possible magnetic field gradient during Zeeman slowing, which breaks the interaction between atoms and laser radiation. For currents below the optimum value, the magnetic field gradient drops and, hence, the cooling efficiency decreases.

We have experimentally investigated the dependence of the flux of cold atoms on the laser radiation intensity I_{laser}. In our experiments, the maximum laser radiation intensity corresponded to a saturation parameter of $G = 30$. A twofold decrease in this value reduces the detected flux of cold atoms approximately by half, while the average velocity of cooled atoms remains unchanged. A fourfold decrease in the value of I_{laser} leads to a significant decrease in the number of cold atoms, while the average velocity of these atoms increases by a factor of about 1.4. This behavior is explained by the fact that the magnetic field profile in the Zeeman slower deviated from the ideal shape. By increasing the laser radiation intensity, it was possible to compensate for the nonideal magnetic field distribution by means of field-induced broadening, which led to a decrease in the average velocity and an increase in the flux of cold atoms. According to the estimates presented above, the imperfect magnetic field distribution can be compensated provided that the atomic transition saturation parameter is $G = 14$. When the saturation parameter for the dominant (cooling) laser mode in our experiments was $G_1 = 14$, the corresponding value for the second laser mode was as small as $G_2 = 3.5$ that was insufficient for the effective Zeeman slowing.

We have also studied the dependence of the Zeeman slowing efficiency on the laser radiation polarization and on the mutual orientation of electric vector **E** and

magnetic field **B**. As expected, any deviations of the laser radiation polarization from the optimum (linear) reduced the efficiency of Zeeman slowing. These deviations lead to a decrease in intensity of the laser radiation component exciting the atomic transitions with $\Delta m = +1$ and, hence, to a drop in the cooling efficiency (Fig. 10).

5. PARAMETERS OF A COLD ATOMIC BEAM

We have determined the main parameters of the cold atomic beam, including the intensity, density, divergence, brightness, and phase space density. The intensity of a beam of cold atoms with an average velocity of 12 m/s (at an atomic source temperature of 250°C) was 3×10^{12} s^{-1}. We studied the possibility of improving this parameter by increasing the source temperature. As the source temperature was increased to 400°C, the cold atomic beam intensity exhibited a growth by a factor of 2.4, but further increase in the source temperature led to a decrease in the beam intensity. This is related to the primary beam depletion of the low-velocity atoms as a result of their scattering from fast atoms. Thus, the maximum intensity of the beam of cold atoms in our experiments was $I_{max} = 7.2 \times 10^{12}$ s^{-1}. The corresponding density of cold atoms was $n_{max} = I_{max}/S\bar{V} \approx 4.7 \times 10^{10}$ cm^{-3}.

The brightness of an atomic beam is defined as

$$R = \frac{I}{\pi(\Delta x_\perp)^2 \Delta \Omega},$$

where $\Delta x_\perp$ is the transverse size of the beam and $\Delta \Omega$ is the solid angle in which atoms are confined. The latter solid angle is determined as $\Delta \Omega = \pi(\Delta V_\perp/\bar{V}_\parallel)^2$, where $\Delta V_\perp$ is the width of the transverse velocity component distribution and $\bar{V}_\parallel$ is the average value of the longitudinal velocity component. The maximum transverse velocity of atoms was determined by the beam-forming diaphragms and amounted to $V_\perp \approx 4.5$ m/s. Therefore, for an average longitudinal velocity of $\bar{V}_\parallel = 12$ m/s, cold atoms move within a solid angle of $\Delta \Omega = 0.14\pi$. For the maximum atomic flux of $I_{max} = 7.2 \times 10^{12}$ s^{-1}, the brightness amounts to $R = 1.3 \times 10^{18}$ (sr m^2 s)$^{-1}$. The spectral brightness of an atomic beam is defined as

$$B_r = R\frac{\bar{p}_\parallel}{\Delta p_\parallel}.$$

In our experiments, the spectral brightness was $B_r = 1.7 \times 10^{18}$ (sr m^2 s)$^{-1}$. The phase space density of an

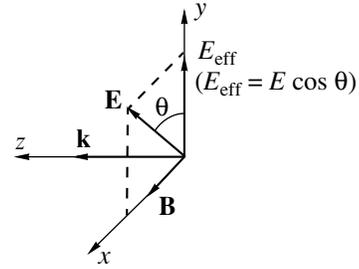**Fig. 10.** Schematic diagram illustrating the influence of the mutual orientation of the magnetic induction **B** and the electric vector **E** of the cooling laser radiation on the Zeeman slowing efficiency.
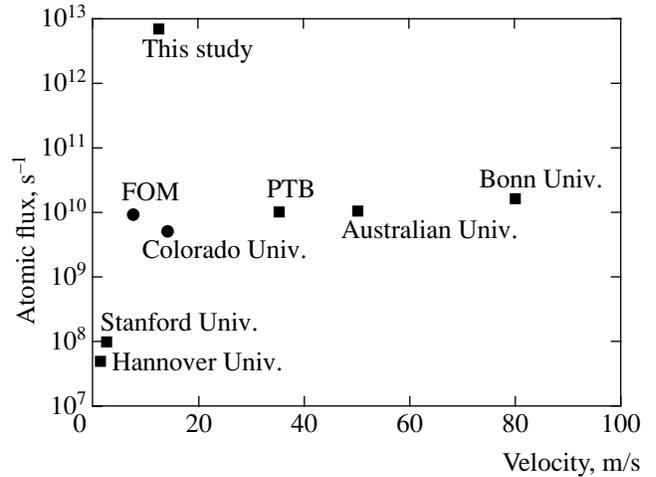

Fig. 11. The flux and average velocity of cooled atoms obtained in this study in comparison to the results obtained by other researchers using cooled atomic beams (■) and atomic beams from 3D-MOT (●): This study; Hannover Univ. [8]; PTB [20]; Australia Univ. [21]; Bonn Univ. [19]; Stanford Univ. [9]; FOM [23];Colorado Univ. [11].

atomic beam is given by the expression

$$\tilde{\Lambda} = B_r \frac{\pi}{m^3 \bar{V}_\parallel^4} h^3.$$

The maximum phase space density observed in our experiments was $\tilde{\Lambda} = 2.4 \times 10^{-11}$.

Figure 11 shows a comparison of the parameters (plotted as the beam intensity versus average atomic velocity) of cold beams obtained in various research centers. As can be seen from these data, the flux of cold atoms achieved in this study is more than two orders of magnitude higher than the beam intensities reported by other researchers. This increase in the total flux of cold atoms has become possible for two reasons: first, due to the implemented scheme with transverse magnetic field, which allowed the length of the cooling tract to be significantly reduced; second, due to the use of an
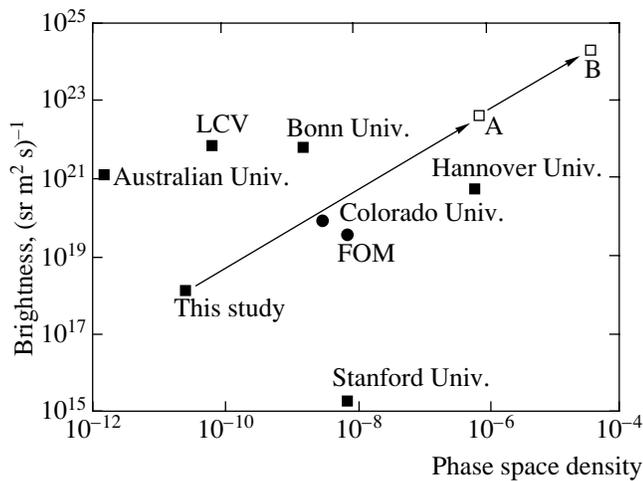
Fig. 12. The brightness and phase space density of cooled atomic beams obtained in this study in comparison to the results obtained by other researchers: This study; Australia Univ. [21]; LCV Univ. [22]; Bonn Univ. [19]; Colorado Univ. [11]; Stanford Univ. [9]; FOM [23]; Hannover Univ. [8]. Arrows show the values of brightness and phase space density of a cold atomic beam predicted for the proposed method in combination with 2D-MOT cooling: (A) for the transverse Doppler cooling; (B) for transverse sub-Doppler cooling.

atomic source providing for an intense primary thermal beam with undepleted low-velocity fraction of the total velocity distribution.

We have estimated the possibility to further increase the level of brightness and phase space density of a cold atomic beam achieved in our experiments. This can be provided by the two-dimensional magnetooptical trap technique (2D-MOT). The density of atoms in a 2D-MOT is limited by the following physical factors: (i) dipole–dipole interaction between atoms; (ii) repulsive potential created by scattered laser radiation; and (iii) attractive potential related to the absorption of laser radiation [18]. The large intensity of a cold beam achieved in our case suggests that the most important factor determining the transverse size and temperature of the beam in the course of transverse laser cooling is reabsorption of photons inside the atomic ensemble. The multiple reabsorption of photons leads to the heating of atoms and to a decrease in the compressive force, so that the maximum possible density of atoms in the beam is restricted to a value on the order of $n_{max} = 10^{12}$ cm^{-3} [18]. Taking into account this limitation and considering the maximum cold beam intensity and the average atomic velocity obtained in our experiments, a minimum possible transverse size that can be achieved by means of the 2D-MOT technique is $\Delta x_\perp \approx 430$ μm. Upon cooling atoms in a 2D-MOT down to the Doppler limit of laser cooling, the angular divergence of the atomic beam is 2×10^{-2} rad, while reaching sub-Doppler temperatures of about 3 μK allows the divergence to be reduced down to 2.7×10^{-3} rad. Therefore, appli-

cation of the 2D-MOT technique in our case will allow the brightness and phase space density to be increased by a factor of 3×10^4 and 1.5×10^6, respectively.

Figure 12 presents a summary of data on the brightness and phase space density of cooled atomic beams obtained in various research centers using the 2D-MOT technique. For the comparison, we have also plotted the brightness and phase space density of the atomic beam obtained in this study, as well as expected values of the phase space density that can be achieved using a 2D-MOT technique in the case of Doppler (point A) and sub-Doppler cooling (point B). As can be seen, our cold beam parameters obtained even without using the 2D-MOT technique are comparable to the analogous parameters achieved due to 2D-MOT. The arrows in Fig. 12 show the calculated values of brightness and phase space density of a cold atomic beam obtained by the proposed method in combination with 2D-MOT. According to Figs. 11 and 12, the proposed method of obtaining cooled atomic beams significantly improves the phase space density of a beam.

6. CONCLUSIONS

Using the method of Zeeman laser cooling in a transverse magnetic field, we obtained a source of cold ^{85}Rb atoms with a beam intensity of 7.2×10^{12} s^{-1} at an average atomic velocity of 12 m/s. The density of cold atoms in the source was 4.7×10^{10} cm^{-3}.

ACKNOWLEDGMENTS

REFERENCES

1. W. Ketterle, Rev. Mod. Phys. **74**, 1131 (2002).

2. J. T. M. Walraven, in *Quantum Dynamics of Simple Systems*, Ed. by G. L. Oppo and S. M. Barnett (Inst. of Phys., London, 1996), p. 315.

3. W. D. Phillips, J. V. Prodan, and H. J. Metcalf, J. Opt. Soc. Am. B **2**, 1751 (1985).

4. T. E. Barrett, S. W. Dapore-Schwartz, M. D. Ray, *et al.*, Phys. Rev. Lett. **67**, 3483 (1991).

5. W. Ertmer, R. Blatt, J. L. Hall, *et al.*, Phys. Rev. Lett. **54**, 996 (1985).

6. W. Ketterle, A. Martin, M. A. Joffe, *et al.*, Phys. Rev. Lett. **69**, 2483 (1992).

7. M. Zhu, C. W. Oates, and J. S. Hall, Phys. Rev. Lett. **67**, 46 (1991).

8. M. Schiffer, M. Christ, G. Wokurka, *et al.*, Opt. Commun. **134**, 423 (1997).

9. E. Riis, D. S. Weiss, K. A. Moler, *et al.*, Phys. Rev. Lett. **64**, 1658 (1990).

10. J. Nellessen, J. Werner, and W. Ertmer, Opt. Commun. **78**, 300 (1990).

11. Z. T. Lu, K. L. Corwin, M. J. Renn, *et al.*, Phys. Rev. Lett. **77**, 3331 (1996).

12. S. N. Bagayev, V. I. Baraulia, A. E. Bonert, *et al.*, Laser Phys. **11**, 1178 (2001).

13. V. S. Letokhov, V. G. Minogin, and B. D. Pavlik, Zh. Éksp. Teor. Fiz. **72**, 1328 (1977) [Sov. Phys. JETP **45**, 698 (1977)].

14. N. F. Ramsey, *Molecular Beams* (Clarendon Press, Oxford, 1956; Inostrannaya Literatura, Moscow, 1960).

15. P. N. Melentiev, M. V. Subbotin, and V. I. Balykin, Laser Phys. **11**, 891 (2001).

16. K. L. Corwin, Z. T. Lu, C. F. Hand, *et al.*, Appl. Opt. **37**, 3295 (1998).

17. R. D. Swenumson and U. Even, Rev. Sci. Instrum. **52**, 559 (1981).

18. V. I. Balykin and V. G. Minogin, Zh. Éksp. Teor. Fiz. **123**, 13 (2003) [JETP **96**, 8 (2003)].

19. F. Lison, P. Schuh, D. Haubrich, *et al.*, Phys. Rev. A **61**, 13405 (2000).

20. A. Witte, T. Kisters, F. Riehle, *et al.*, J. Opt. Soc. Am. B **9**, 1030 (1992).

21. M. D. Hoogerland, D. Milic, W. Lu, *et al.*, Aust. J. Phys. **49**, 567 (1996).

22. W. Rooijakkers, W. Hogervorst, and W. Vassen, Opt. Commun. **123**, 321 (1996).

23. K. Dieckmann, R. J. C. Spreeuw, M. Weidenmuller, *et al.*, Phys. Rev. A **58**, 3891 (1998).

Translated by P. Pozdeev